nature immunology



# Fever-range thermal stress promotes lymphocyte trafficking across high endothelial venules via an interleukin 6 *trans*-signaling mechanism

Qing Chen[1], Daniel T Fisher[1], Kristen A Clancy[1], Jean-Marc M Gauguet[2], Wan-Chao Wang[1], Emily Unger[1], Stefan Rose-John[3], Ulrich H von Andrian[2], Heinz Baumann[4] & Sharon S Evans[1]

**Fever is an evolutionarily conserved response during acute inflammation, although its physiological benefit is poorly understood. Here we show thermal stress in the range of fever temperatures increased the intravascular display of two 'gatekeeper' homing molecules, intercellular adhesion molecule 1 (ICAM-1) and CCL21 chemokine, exclusively in high endothelial venules (HEVs) that are chief portals for the entry of blood-borne lymphocytes into lymphoid organs. Enhanced endothelial expression of ICAM-1 and CCL21 was linked to increased lymphocyte trafficking across HEVs. A bifurcation in the mechanisms controlling HEV adhesion was demonstrated by evidence that the thermal induction of ICAM-1 but not of CCL21 involved an interleukin 6 *trans*-signaling pathway. Our findings identify the 'HEV axis' as a thermally sensitive alert system that heightens immune surveillance during inflammation by amplifying lymphocyte trafficking to lymphoid organs.**

The continuous recirculation of lymphocytes across specialized high endothelial venules (HEVs) in lymphoid organs is critical for the maintenance of immune homeostasis and immune surveillance. HEVs lined by cuboidal endothelial cells are distinguished from flat-walled vascular beds throughout the body by their ability to support efficient extravasation of lymphocytes into underlying tissues[1]. Lymphocyte entry across HEVs involves a highly ordered sequence of adhesion events that includes tethering and rolling along vessel walls; chemokine-dependent activation; firm arrest; and transendothelial migration[2–4].

Primary tethering and rolling of naive and central memory lymphocytes in HEVs of peripheral lymph nodes (PLNs) and mesenteric lymph nodes (MLNs) is initiated via the engagement of sialomucin-like endothelial molecules, collectively called 'peripheral lymph node addressin' (PNAd), by L-selectin on lymphocytes[2,3,5]. Mucosal addressin cell adhesion molecule 1 (MAdCAM-1) on HEVs of MLNs and Peyer's patches also supports primary adhesion through interactions with L-selectin or $\alpha_4\beta_7$ integrin on circulating lymphocytes[2]. Secondary firm arrest is triggered mainly by interactions between CCL21 chemokine displayed on the lumenal surfaces of HEVs with $G_{\alpha i1}$ protein–coupled CCR7 chemokine receptors on lymphocytes[2–4]. Chemokine activation increases the affinity of leukocyte function–associated antigen 1 (LFA-1) for its endothelial ligands, intercellular adhesion molecule 1 (ICAM-1) and ICAM-2, which have redundant functions during steady-state trafficking across HEVs[2,3]. The final process of transendothelial migration in HEVs is not fully understood, but is suggested by *in vitro* models to involve molecules located in interendothelial junctions, including ICAM-1, ICAM-2, CD31 and junctional adhesion molecules 1 and 2 (refs. 3,6).

Local and systemic increases in temperature are cardinal features of inflammation. The evolutionarily conserved febrile response has been linked to improved survival during infection in endothermic and ectothermic species[7–10]. A key unresolved issue relates to the physiological benefit of fever. Studies have suggested that febrile temperatures provide a 'danger signal' that mobilizes the entry of blood-borne lymphocytes into secondary lymphoid organs, where the probability of encountering cognate antigens or pathogens is enhanced. Temperatures that mimic febrile episodes (38–40 °C) act directly on T lymphocytes and B lymphocytes to enhance L-selectin-dependent and $\alpha_4\beta_7$ integrin–dependent homing across lymph node and Peyer's patch HEVs[11–13]. Thermal modulation of L-selectin adhesion involves a tightly orchestrated *trans*-signaling mechanism initiated by engagement of the glycoprotein gp130 signal-transducing subunit by interleukin 6 (IL-6) and a soluble form of the IL-6 receptor-α binding subunit (sIL-6Rα)[13]. Those findings support the present view that IL-6 *trans* signaling provides a molecular 'switch' that governs lymphocyte trafficking during acute inflammation or chronic inflammatory disorders[14,15].

Although febrile temperatures can improve the vascular delivery of inflammatory cells to tissues by regulating hemodynamic parameters

[1]Departments of Immunology, Roswell Park Cancer Institute, Buffalo, New York 14263, USA. [2]The CBR Institute for Biomedical Research and Department of Pathology, Harvard Medical School, Boston, Massachusetts, 02115, USA. [3]Department of Biochemistry, Christian Albrechts University Kiel, D-24098 Kiel, Germany. [4]Molecular and Cellular Biology, Roswell Park Cancer Institute, Buffalo, New York 14263, USA. Correspondence should be addressed to S.S.E. (sharon.evans@roswellpark.org).

Received 19 June; accepted 4 October; published online 5 November 2006; corrected online 10 November 2006 (details online); doi:10.1038/ni1406

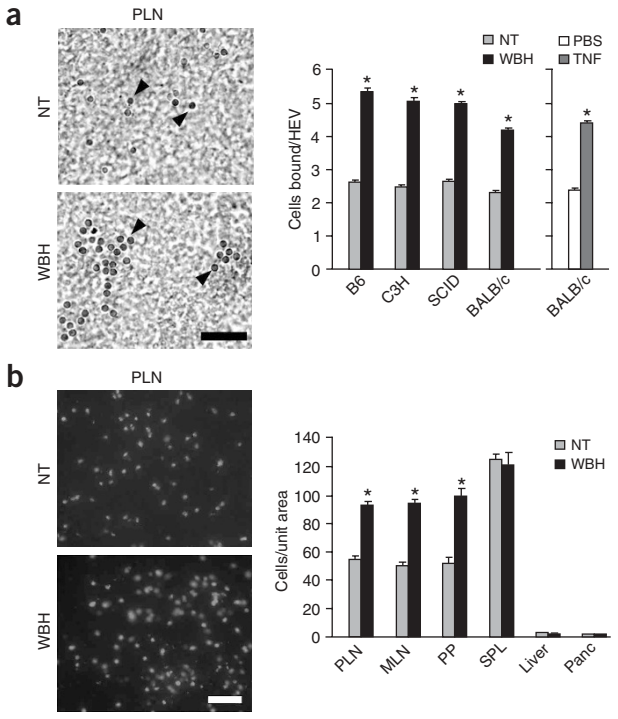


**Figure 1** Fever-range thermal stress enhances HEV adhesion and homing of lymphocytes to lymphoid organs with HEV structures. (**a**) *In vitro* frozen-section adherence assay of the binding of splenocytes to HEVs in pooled PLNs from individual normothermic control mice (NT), WBH-treated mice or TNF-treated mice. Arrowheads in representative photomicrographs (left) indicate toluidine-stained splenocytes bound to individual HEVs in PLNs from BALB/c mice. Right, quantification (mean ± s.e.m.) of cells bound to HEVs ($n = 3 \times 10^2$ HEVs per mouse). B6, C57BL/6; SCID, severe combined immunodeficiency. (**b**) *In vivo* short-term (1-hour) homing of fluorescence-labeled splenocytes to secondary lymphoid organs (pooled PLNs, MLNs, Peyer's patches (PP) and spleen (SPL)) and nonlymphoid organs (liver and pancreas (Panc)) in individual normothermic control BALB/c mice or WBH-treated BALB/c mice. Left, representative photomicrographs of PLNs. Right, quantification (mean ± s.e.m.) of calcein-labeled cells in organ cryosections, by fluorescence microscopy ($n = 10$ fields per mouse). *, $P < 0.0001$, NT versus WBH. Scale bars (**a**,**b**), 50 μm. Data are representative of three or more (**a**) or ten (**b**) independent experiments.

such as vasodilation and blood flow, the contribution of thermal stress to endothelial adhesion remains mostly unexplored. The binding function of 'gatekeeper' cuboidal HEVs is augmented by thermal stress in the range of fever temperatures *in vivo*[16,17], whereas febrile temperatures do not influence the ability of squamous endothelium of nonlymphoid organs to support leukocyte adhesion *in vivo* or *in vitro*[16,18,19]. Here we report that the thermal element of fever controls the molecular mechanisms that underlie firm adhesion and transendothelial migration of blood-borne lymphocytes across HEVs. We identified an integrated function for IL-6 *trans* signaling as a regulator of trafficking by demonstrating that IL-6–sIL-6Rα mediated thermal induction of ICAM-1-dependent extravasation of lymphocytes selectively in HEVs of lymphoid organs. Our results support the idea that HEVs act as sentinels during febrile inflammatory responses by heightening trafficking of naive and central memory lymphocytes to secondary lymphoid organs.

## RESULTS

### Thermal stress stimulates lymphocyte-HEV interactions

We used several experimental approaches to assess the effects of thermal stress on HEV adhesion independently of other factors that may also influence trafficking, such as hemodynamic parameters. In the first series of studies, we treated mice for 6 h with whole-body hyperthermia (WBH) to raise the core temperature to the range of fever temperatures ('fever-range'; 39.5 ± 0.5 °C). We quantified the binding activity of individual HEVs by an *in vitro* assay in which we allowed splenocytes (from untreated mice) to adhere to HEVs in PLN

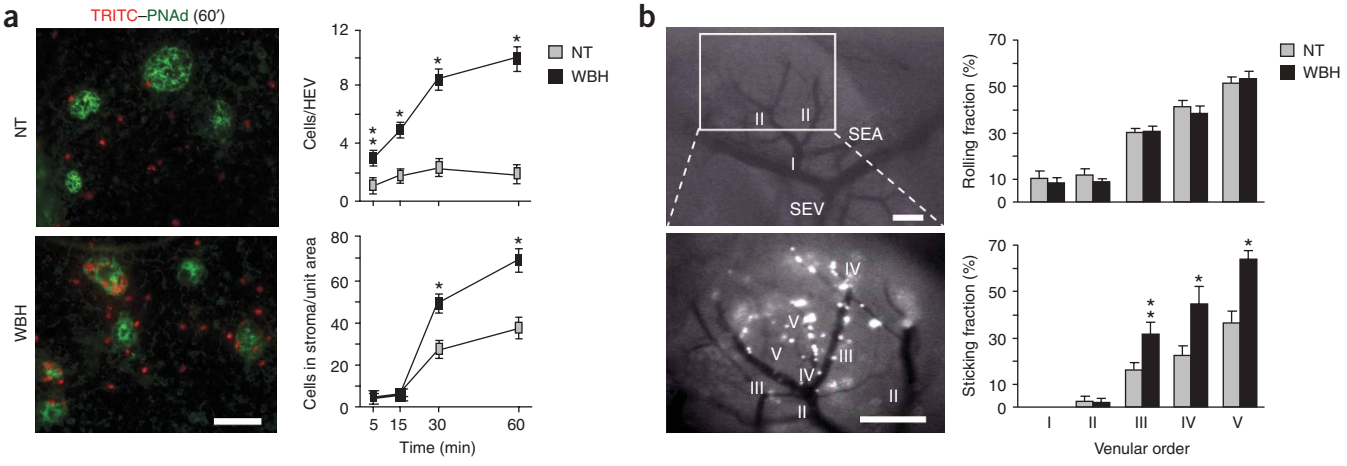


**Figure 2** Fever-range thermal stress enhances lymphocyte-HEV interactions. (**a**) Kinetic analysis of lymphocyte homing. PLNs were isolated 5–60 min after adoptive transfer of TRITC-labeled splenocytes (red) into normothermic control BALB/c mice or WBH-treated BALB/c mice. Tissue cryosections (left) are stained with mAb specific for PNAd to visualize HEVs (green) and are representative photomicrographs of TRITC-labeled cells associated with HEVs or infiltrated into the tissue parenchyma at 60 min (60'); right, quantification of those cells by fluorescence microscopy. Data (mean ± s.e.m.) are of ten fields analyzed of pooled PLNs from individual mice and are representative of three or more independent experiments. (**b**) Intravital microscopy (left) of the interactions of calcein-labeled splenocytes with the lymph node venular tree of a WBH-treated mouse, showing the vascular structure, including the superficial epigastric artery (SEA), superficial epigastric vein (SEV) and venular branches (I–V) in an inguinal lymph node (**Supplementary Video 1** online). Right, rolling fractions and sticking fractions in normothermic control and WBH-treated C57BL/6 mice. Data (mean ± s.e.m.) are from three mice per treatment group in three independent experiments. Scale bars, 50 μm (**a**) or 200 μm (**b**). *, $P < 0.0001$, and **, $P < 0.01$, normothermic versus WBH.

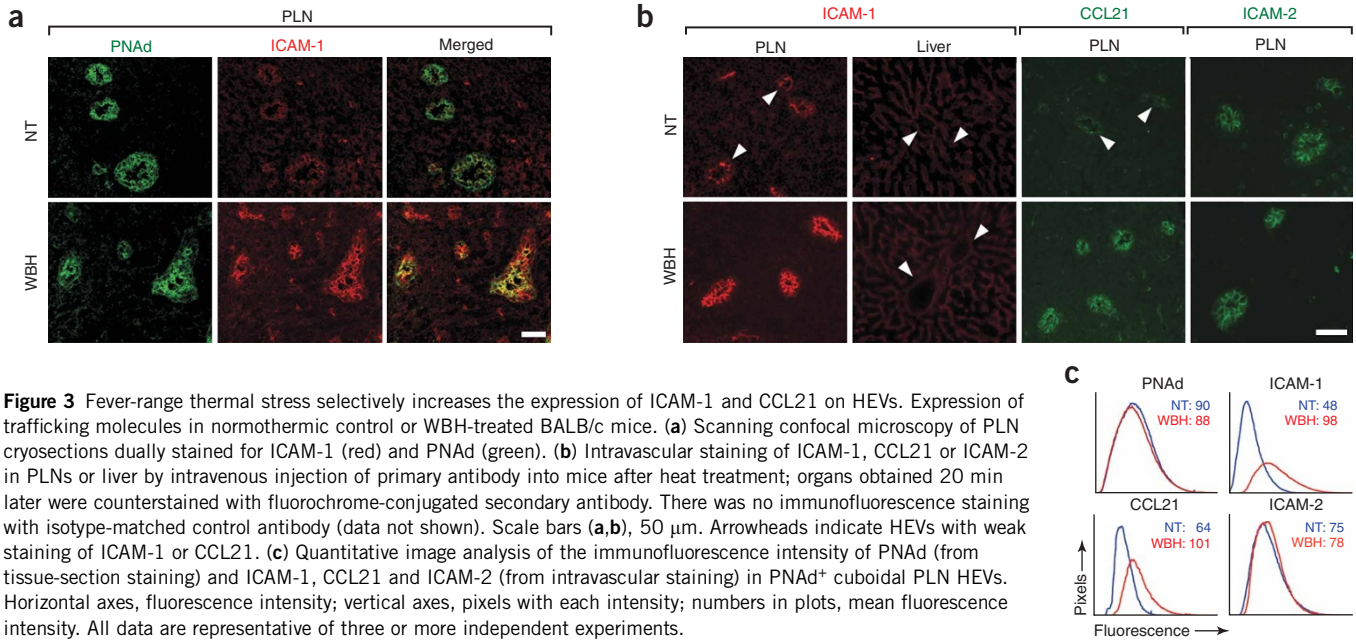


**Figure 3** Fever-range thermal stress selectively increases the expression of ICAM-1 and CCL21 on HEVs. Expression of trafficking molecules in normothermic control or WBH-treated BALB/c mice. (**a**) Scanning confocal microscopy of PLN cryosections dually stained for ICAM-1 (red) and PNAd (green). (**b**) Intravascular staining of ICAM-1, CCL21 or ICAM-2 in PLNs or liver by intravenous injection of primary antibody into mice after heat treatment; organs obtained 20 min later were counterstained with fluorochrome-conjugated secondary antibody. There was no immunofluorescence staining with isotype-matched control antibody (data not shown). Scale bars (**a**,**b**), 50 μm. Arrowheads indicate HEVs with weak staining of ICAM-1 or CCL21. (**c**) Quantitative image analysis of the immunofluorescence intensity of PNAd (from tissue-section staining) and ICAM-1, CCL21 and ICAM-2 (from intravascular staining) in PNAd$^+$ cuboidal PLN HEVs. Horizontal axes, fluorescence intensity; vertical axes, pixels with each intensity; numbers in plots, mean fluorescence intensity. All data are representative of three or more independent experiments.



organ cryosections from control mice at normal temperature ('normothermic' mice) or heat-treated mice. Fever-range WBH increased the ability of PLN HEVs to support lymphocyte adhesion in several immunocompetent mouse strains (C57BL/6, C3H and BALB/c) as well as in mice with severe combined immunodeficiency that lacked B lymphocytes and T lymphocytes (**Fig. 1a**). We detected similar increases in HEV adhesion in response to thermal stress or to the administration of recombinant tumor necrosis factor (TNF; **Fig. 1a**), a potent stimulator of vascular adhesion *in vitro* and *in vivo*[20].

We next examined the thermal regulation of lymphocyte trafficking in short-term (1-hour) *in vivo* homing assays in which we labeled splenocytes *ex vivo* with fluorescent tracking dyes (TRITC or calcein) and then injected the cells intravenously into normothermic control or WBH-treated BALB/c mice. We allowed recipient mice to equilibrate to normal body temperature before adoptively transferring labeled cells to reverse the thermal effects on blood flow and to avoid heat activation of L-selectin or $\alpha_4\beta_7$ integrin adhesion in labeled indicator cells[11–13]. Thermal stress caused an increase of approximately twofold in the trafficking of labeled cells selectively in secondary lymphoid organs with HEVs (PLNs, MLNs and Peyer's patches) but not in spleen or extralymphoid organs (such as liver or pancreas), which lack HEV structures (**Fig. 1b** and **Supplementary Fig. 1** online). WBH treatment did not alter the composition of cells that trafficked to PLNs, suggesting that homeostatic trafficking mechanisms were maintained. Thus, thermal stress did not result in enrichment for specific leukocyte populations that gained entry to PLNs, including T cells (CD4$^+$ and CD8$^+$) that traffic more efficiently than B cells (B220$^+$)[21,22], or monocytes (CD11b$^{hi}$Gr1$^{lo}$) and neutrophils (Gr1$^{hi}$), which were essentially excluded[2,3] (**Supplementary Fig. 1**). Naive cells (L-selectin-high CD44$^{lo}$) or central memory cells (L-selectin-high CD44$^{hi}$) constituted the main T cell subsets that homed to PLNs in control and hyperthermic conditions, whereas effector-memory T cells (L-selectin-low CD44$^{hi}$; **Supplementary Fig. 1**) and activated T cell populations (L-selectin-low CXCR3$^{hi}$CCR7$^{lo}$; data not shown) were excluded from this site.

We assessed the influence of thermal stress on the kinetics of lymphocyte interactions with gatekeeper HEVs after intravenous injection of fluorescence-labeled splenocytes into normothermic or WBH-treated mice. We counterstained tissue sections with monoclonal antibodies (mAbs) specific for molecules on PLN HEVs (PNAd) or Peyer's patch HEVs (MAdCAM-1) to determine whether labeled cells were located in HEVs or were extravasated into the tissue parenchyma. We found that WBH treatment increased the number of lymphocytes associated with PLN HEVs (**Fig. 2a**) and Peyer's patch HEVs (**Supplementary Fig. 2** online) within 5 min of transfer and that the increase in lymphocyte-HEV interactions was sustained over 1 h. Notably, more lymphocytes completed the multistep process culminating in extravasation into the stroma of PLNs or Peyer's patches by 30 min in WBH-treated mice than in normothermic control mice at 1 h ($P < 0.002$; **Fig. 2a** and **Supplementary Fig. 2**).

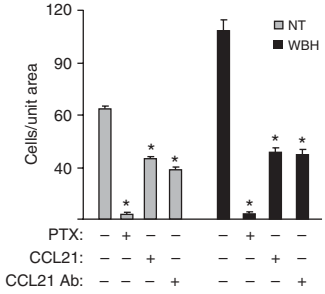


**Figure 4** CCL21 is required for the thermal stimulation of lymphocyte trafficking across HEVs. Short-term (1-hour) homing of TRITC-labeled splenocytes. Cells were pretreated with (+) or without (–) pertussis toxin (PTX) or were pretreated with (+) or without (–) a desensitizing concentration of CCL21 before adoptive transfer into normothermic control or WBH-treated BALB/c mice. Alternatively, mice were treated for 20 min with (+) or without (–) CCL21-neutralizing antibody (CCL21 Ab) before cell transfer. Isotype-matched control antibody did not affect lymphocyte homing (data not shown). Cryosections of pooled PLNs from individual mice were counterstained for PNAd, and TRITC-labeled cells infiltrating the parenchyma were quantified by fluorescence microscopy ($n = 10$ fields per mouse). *, $P < 0.0001$, function-blocking reagent versus untreated control. Data (mean ± s.e.m.) are representative of three or more independent experiments.

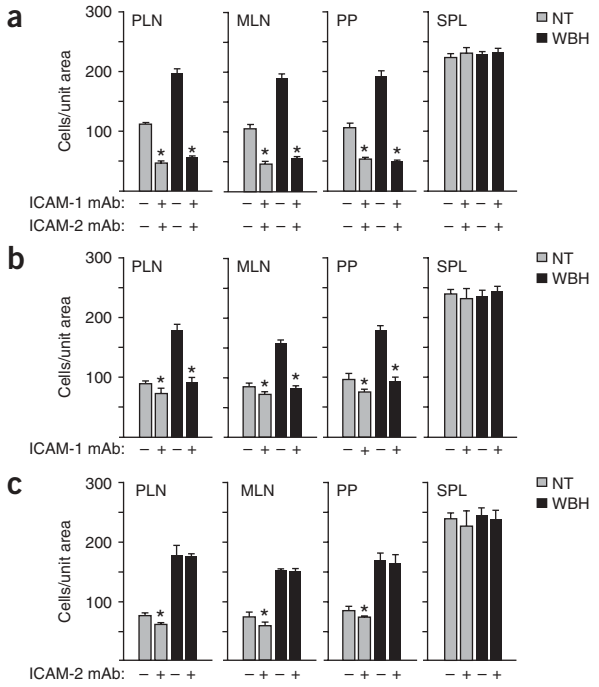


**Figure 5** ICAM-1 is required for the thermal enhancement of trafficking across HEVs. Short-term (1-hour) homing of TRITC-labeled splenocytes in normothermic control or WBH-treated BALB/c mice. At 20 min before adoptive transfer, recipient mice were treated with function-blocking mAbs (+) specific for ICAM-1 and ICAM-2 (**a**) or for ICAM-1 only (**b**) or ICAM-2 only (**c**) or with isotype-matched control antibody (–). TRITC-labeled cells in tissue cryosections from individual mice were quantified by fluorescence microscopy ($n = 10$ fields per mouse). *, $P < 0.0001$, function-blocking mAb versus control antibody. Data (mean ± s.e.m.) are representative of three or more independent experiments.

We used intravital microscopy of inguinal lymph nodes to pinpoint the nature of the adhesive interactions regulated by thermal stress (**Fig. 2b**). High-order (III–V) postcapillary HEVs detected in this organ preparation reside in the paracortical region, whereas low-order (I and II) flat-walled venules drain into the superficial epigastric vein in the medulla[23]. WBH pretreatment did not affect the frequency of rolling interactions throughout the venular tree (**Fig. 2b**). However, heat treatment substantially increased the fraction of cells that transitioned from primary rolling to secondary firm sticking exclusively in order III–V venules (HEVs). The velocity of noninteracting lymphocytes in order III venules was equivalent in normothermic and WBH-treated mice (1,195 ± 340 μm/s and 1,130 ± 549 μm/s, respectively (mean ± s.e.m.); $n > 60$ cells analyzed in three experiments), indicating that the increase in sticking interactions could not be attributed to sustained effects of heat pretreatment on blood flow. Thus, thermal stimulation of lymphocyte homing in lymphoid organs is correlated with enhanced secondary firm adhesive interactions selectively in HEVs.

### Thermal stress enhances ICAM-1 and CCL21 display in HEVs

To investigate the molecular basis of the thermal stimulation of lymphocyte-HEV interactions, we examined the expression of trafficking molecules known to participate in the multistep adhesion sequence in HEVs. Two-color confocal immunofluorescence microscopy of tissue cryosections showed that fever-range thermal stress did not alter the relative expression of PNAd or MAdCAM-1, which mediate primary tethering and rolling in PLN or Peyer's patch HEVs, respectively (**Fig. 3a** and **Supplementary Fig. 2**). In contrast, the expression of ICAM-1, which participates in secondary adhesion and transendothelial migration, was enhanced considerably by heat in PNAd$^+$ and MAdCAM-1$^+$ HEVs (**Fig. 3a** and **Supplementary Fig. 2**). We detected similar ICAM-1 staining in HEVs after thermal stress or systemic administration of recombinant TNF (**Supplementary Table 1** online). Although TNF treatment upregulated ICAM-1 indiscriminately on the vessels of all organs examined, the response to thermal stress was site specific, such that only HEVs of lymphoid

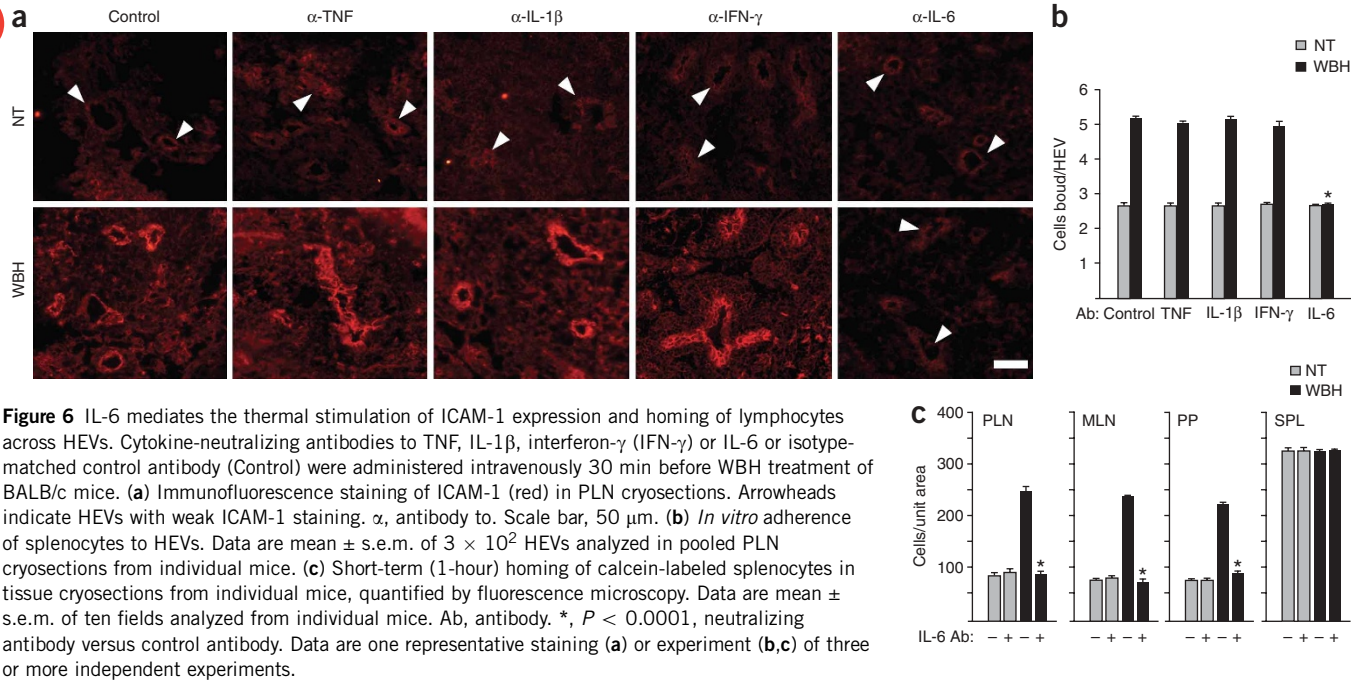


**Figure 6** IL-6 mediates the thermal stimulation of ICAM-1 expression and homing of lymphocytes across HEVs. Cytokine-neutralizing antibodies to TNF, IL-1β, interferon-γ (IFN-γ) or IL-6 or isotype-matched control antibody (Control) were administered intravenously 30 min before WBH treatment of BALB/c mice. (**a**) Immunofluorescence staining of ICAM-1 (red) in PLN cryosections. Arrowheads indicate HEVs with weak ICAM-1 staining. α, antibody to. Scale bar, 50 μm. (**b**) *In vitro* adherence of splenocytes to HEVs. Data are mean ± s.e.m. of $3 \times 10^2$ HEVs analyzed in pooled PLN cryosections from individual mice. (**c**) Short-term (1-hour) homing of calcein-labeled splenocytes in tissue cryosections from individual mice, quantified by fluorescence microscopy. Data are mean ± s.e.m. of ten fields analyzed from individual mice. Ab, antibody. *, $P < 0.0001$, neutralizing antibody versus control antibody. Data are one representative staining (**a**) or experiment (**b**,**c**) of three or more independent experiments.

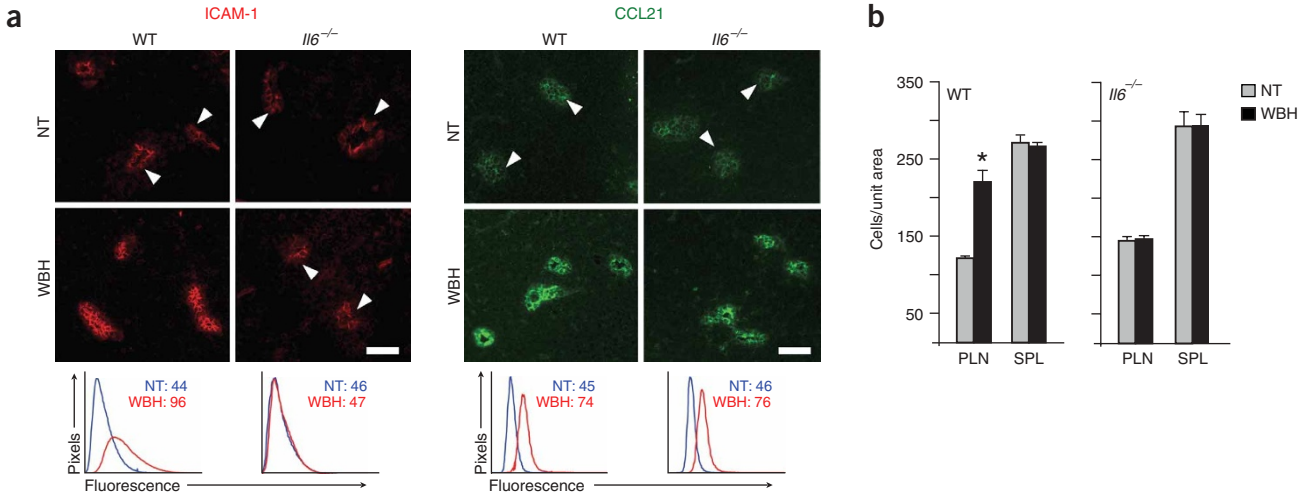


**Figure 7** Thermal induction of ICAM-1 and lymphocyte homing does not occur in IL-6-deficient mice. (**a**) Intravascular staining of ICAM-1 (red) and CCL21 (green) in PLNs from normothermic control or WBH-treated *Il6*$^{-/-}$ and wild-type (WT) C57BL/6 mice. Arrowheads indicate HEVs with weak staining of ICAM-1 or CCL21. Scale bars, 50 μm. Bottom, quantitative image analysis of ICAM-1 and CCL21 staining: horizontal axes, fluorescence intensity; vertical axes, pixels with each intensity; numbers in plots, mean fluorescence intensity. (**b**) Short-term (1-hour) homing of TRITC-labeled splenocytes in tissue cryosections from individual *Il6*$^{-/-}$ and wild-type mice with (WBH) or without (NT) WBH treatment, quantified by fluorescence microscopy. Data are mean ± s.e.m. of ten fields analyzed from individual mice. *, $P < 0.0001$, NT versus WBH. All data are representative of three or more independent experiments.



organs had increased ICAM-1 expression (**Supplementary Table 1**). WBH treatment did not alter the vascular expression of other adhesion molecules that mediate transendothelial migration, including CD31 (**Supplementary Table 1**) and junctional adhesion molecules 1 and 2 (data not shown). Thermal stress also did not modify the HEV expression of molecules associated with inflammatory responses, such as vascular cell adhesion molecule 1 (**Supplementary Table 1**), E-selectin and Duffy antigen–related receptor for chemokines (data not shown), which has been linked to regulation of the activity and/or availability of inflammatory chemokines (CXCL1, CXCL5, CCL2, CCL5 and CCL7) but not of homeostatic chemokines (CCL21, CCL19, CXCL12 and CXCL13)[3,4,24].

We did intravascular staining *in situ* by injecting ICAM-1-specific mAb into the vascular compartments of recipient mice, then counterstaining tissue sections with fluorescence-labeled detection antibody. Hyperthermia augmented ICAM-1 expression on the lumenal and junctional surfaces of high endothelial cells (HECs; **Fig. 3b**), which are the contact sites for blood-borne lymphocytes undergoing firm adhesion or transendothelial migration. Thermal stress also substantially increased intravascular presentation of the homeostatic chemokine CCL21 (**Fig. 3b**), the principal chemokine required for the transition of lymphocytes from primary rolling interactions to secondary arrest in HEVs, without affecting the weak-to-nondetectable staining for other homeostatic chemokines (CCL19, CXCL12 and CXCL13) on HEVs (data not shown). Quantitative image analysis showed that thermal stress increased the mean fluorescence staining intensity for ICAM-1 and CCL21 on PNAd$^{+}$ cuboidal HEVs by about 2-fold and 1.5-fold, respectively, whereas PNAd and ICAM-2 staining was unchanged (**Fig. 3c**). The finding that the intravascular density of ICAM-2 was not altered established that WBH pretreatment did not generally increase the access of mAbs to epitopes in the HEV microcompartment (**Fig. 3b,c**). There was no change in the lumenal presentation of ICAM-1 (**Fig. 3b**) or CCL21 (data not shown) on the vessels of extralymphoid organs such as liver. Consistent with the observation that thermal stress altered ICAM-1 and CCL21 expression only in HECs that constitute a minor population in nodal tissues (less than 4% of stromal cell–rich fractions[25]), we did not detect a change in the total amounts of those proteins in whole-PLN lysates (**Supplementary Fig. 3** online). These data suggested that increased intravascular display of CCL21 and ICAM-1 contributes to enhanced lymphocyte trafficking across HEVs in response to thermal stress.

## Enhanced homing depends on CCL21 and ICAM-1

We used a 'multipronged' approach to determine the relative contributions of CCL21 and its ligand, CCR7, to improved trafficking by thermal stress. We initially used pertussis toxin, an irreversible inhibitor of $G_{\alpha i}$ protein signaling, to globally inhibit chemokine-dependent entry of lymphocytes into lymphoid organs. Pretreatment of fluorescence-labeled splenocytes with pertussis toxin fully blocked their ability to extravasate in PLNs in both normothermic and hyperthermic conditions (**Fig. 4**). To directly target the CCR7 chemokine receptor for CCL21, we pre-exposed fluorescence-labeled splenocytes to a high concentration of recombinant CCL21 (10 μg/ml) *ex vivo* before transfer into recipient mice (**Fig. 4**). That treatment did not alter the surface expression of L-selectin or LFA-1 on lymphocytes (data not shown). As reported before[26], CCR7 desensitization by that strategy reduced the homing of lymphocytes to PLNs (**Fig. 4**) and Peyer's patches (data not shown) in normothermic conditions, albeit only partially, which probably reflected incomplete desensitization or resensitization *in vivo*. The extent of reduction in lymphocyte trafficking was similar in normothermic and WBH-pretreated mice, indicating a common CCR7-dependent mechanism during trafficking across HEVs in both temperature conditions. Lymphocyte extravasation in control and heat-treated mice was also reduced substantially by a complementary strategy targeting CCL21 *in vivo* with a function-blocking antibody (**Fig. 4**). We conclude that CCR7-CCL21 is the main chemokine receptor–chemokine pair responsible for improved lymphocyte entry across HEVs in response to thermal stress.

Those observations raised the issue of whether CCL21 induction by thermal stress was the sole determinant of physiological importance for homing in HEVs or if heat-inducible ICAM-1 contributed to this

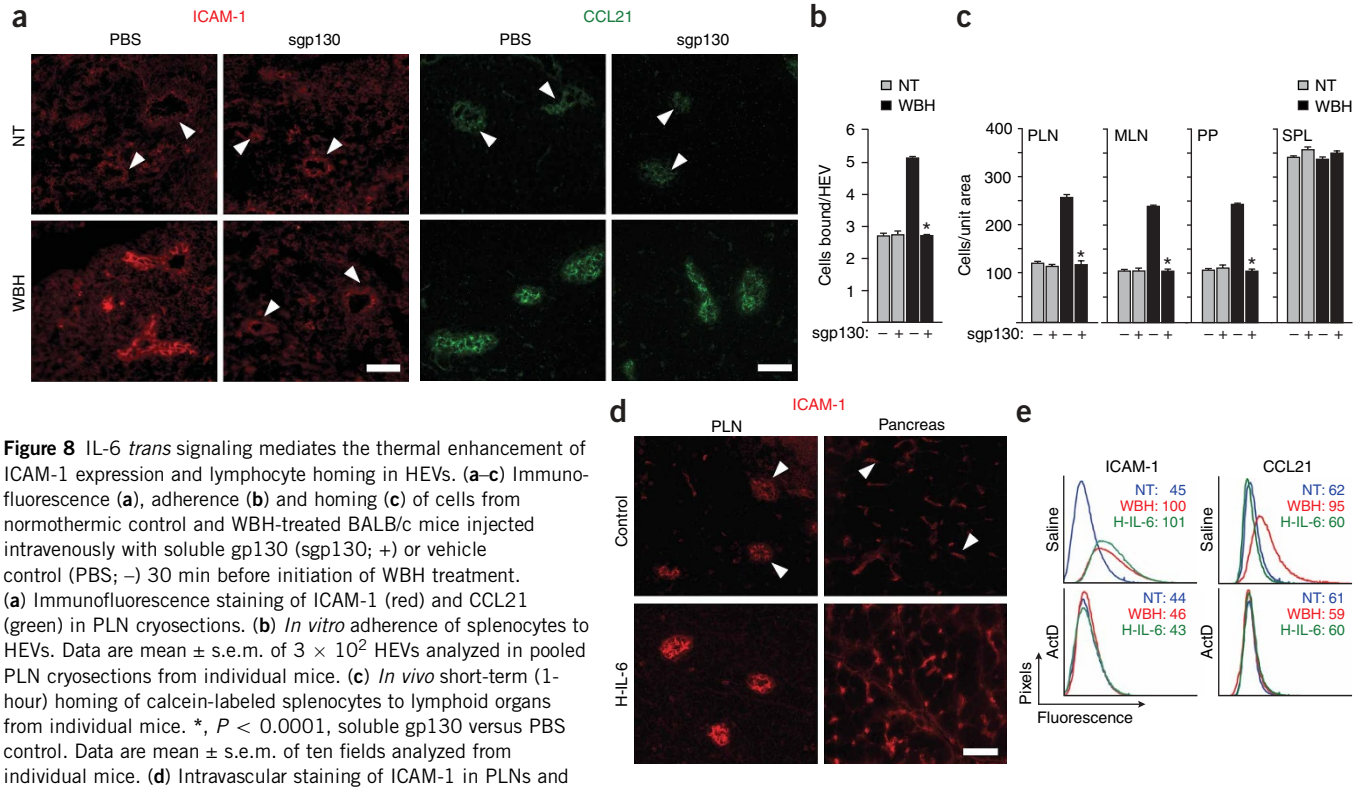


**Figure 8** IL-6 *trans* signaling mediates the thermal enhancement of ICAM-1 expression and lymphocyte homing in HEVs. (**a**–**c**) Immunofluorescence (**a**), adherence (**b**) and homing (**c**) of cells from normothermic control and WBH-treated BALB/c mice injected intravenously with soluble gp130 (sgp130; +) or vehicle control (PBS; –) 30 min before initiation of WBH treatment. (**a**) Immunofluorescence staining of ICAM-1 (red) and CCL21 (green) in PLN cryosections. (**b**) *In vitro* adherence of splenocytes to HEVs. Data are mean ± s.e.m. of $3 \times 10^2$ HEVs analyzed in pooled PLN cryosections from individual mice. (**c**) *In vivo* short-term (1-hour) homing of calcein-labeled splenocytes to lymphoid organs from individual mice. *, $P < 0.0001$, soluble gp130 versus PBS control. Data are mean ± s.e.m. of ten fields analyzed from individual mice. (**d**) Intravascular staining of ICAM-1 in PLNs and pancreata from BALB/c mice treated with hyper-IL-6 (H-IL-6) and from control BALB/c mice. (**e**) Image analysis quantification of the intravascular staining intensity of ICAM-1 and CCL21 in HEVs of pooled PLNs from individual BALB/c mice given actinomycin D (ActD) or vehicle control (Saline) intraperitoneally 30 min before treatment for 6 h with WBH or hyper-IL-6. Horizontal axes, fluorescence intensity; vertical axes, pixels with each intensity; numbers in plots, mean fluorescence intensity. Arrowheads (**a**,**d**) indicate HEVs with weak staining of ICAM-1 or CCL21; scale bars (**a**,**d**), 50 μm. Data are one representative staining (**a**,**d**) or experiment (**b**,**c**,**e**) of three or more independent experiments.

process. We addressed that issue by assessing the relative requirements for LFA-1 and its cognate receptors, ICAM-1 and ICAM-2, in short-term homing studies. Combined mAb blockade of ICAM-1 and ICAM-2 reduced lymphocyte trafficking across HEVs considerably in both normothermic and hyperthermic conditions (**Fig. 5a**), paralleling results obtained with an LFA-1-blocking mAb (data not shown). Independent mAb blockade of ICAM-1 or ICAM-2 had only modest effects on trafficking to lymphoid organs in normothermic conditions (**Fig. 5b,c**), supporting reports that those molecules can substitute for each other as HEV ligands for LFA-1 during steady-state homing in HEVs[27,28]. Interference with ICAM-1 activity, either by neutralizing mAb (**Fig. 5b**) or by genetic targeting in ICAM-1-deficient mice (**Supplementary Fig. 4** online), completely prevented the thermal stimulation of trafficking to PLNs, MLNs and Peyer's patches. In contrast, functional inhibition of ICAM-2 failed to reduce trafficking across HEVs in WBH-treated mice (**Fig. 5c**). We confirmed the requirement for ICAM-1 in heat-induced HEV adhesion by a frozen-section *in vitro* adherence assay (**Supplementary Fig. 4**). Although this assay mainly measures PNAd-dependent adhesion in PLN HEVs in normal conditions[5], LFA-1–ICAM–dependent binding interactions have been characterized in HEVs of inflamed lymph nodes with this method[29]. Evidence that HEVs of control and hyperthermia-treated mice supported equivalent PNAd-dependent adhesion after concomitant blockade of ICAM-1 and ICAM-2 in frozen-section assays (**Supplementary Fig. 4**) was consistent with intravital studies (**Fig. 2b**) demonstrating that thermal stress did not augment primary adhesive interactions in HEVs. These results collectively demonstrated that ICAM-1 is the 'preferential' binding partner for LFA-1 in HEVs in thermal conditions and that high-density presentation of CCL21 is not sufficient, in the absence of ICAM-1, to support improved trafficking to lymphoid organs.

## IL-6 *trans* signaling mediates enhanced trafficking

Inflammatory cytokines, including TNF, IL-1β, interferon-γ and IL-6, are potent stimulators of endothelial expression of ICAM-1 and inflammatory chemokines *in vitro* or *in vivo*[30] (**Supplementary Table 1**). To determine if those candidate cytokines regulate HEV adhesion during thermal stress, we treated mice with cytokine-neutralizing mAbs before initiating WBH and then examined expression of ICAM-1 or CCL21 by HEVs. There was thermal induction of ICAM-1 in PLN HEVs (**Fig. 6a**) and Peyer's patch HEVs (data not shown), despite the presence of mAbs specific for TNF, IL-1β or interferon-γ, whereas there was no induction in mice treated with an IL-6 function–blocking mAb. Similarly, only IL-6-neutralizing mAb blocked the thermal enhancement of HEV adhesion detected by frozen-section *in vitro* adherence assays (**Fig. 6b**). The IL-6-neutralizing mAb also prevented the thermal stimulation of lymphocyte homing across HEVs in PLNs, MLNs and Peyer's patches (**Fig. 6c**). Improved trafficking was not accompanied by a measurable increase in total nodal content of IL-6 during heat treatment (IL-6 in PLNs of normothermic control mice and in mice after WBH treatment at 2, 4 and 6 h: 1.1 ± 0.2 pg/mg total protein, 0.9 ± 0.2 pg/mg total protein, 0.6 ± 0.1 pg/mg total protein and 1.0 ± 0.2 pg/mg total protein, respectively (mean ± s.e.m.); $n = 3$ mice). We confirmed the requirement for IL-6 in IL-6-deficient mice, as thermal stress failed to induce ICAM-1 expression or lymphocyte trafficking in HEVs in

these mice (**Fig. 7a**,**b**). In contrast, IL-6-deficient mice (**Fig. 7a**) and wild-type mice treated with IL-6-neutralizing mAb (data not shown) had normal CCL21 induction in response to thermal stress.

IL-6 regulation of ICAM-1 occurs in primary venular endothelial cells *in vitro* that lack the membrane form of the IL-6Rα binding subunit by means of a *trans*-signaling mechanism that depends on the availability of both IL-6 and a soluble form of IL-6Rα[14,31,32]. To test whether IL-6 *trans* signaling contributes to ICAM-1-mediated homing during thermal stress *in vivo*, we administered recombinant soluble gp130 before WBH treatment. Soluble gp130 competitively inhibits *trans* signaling by IL-6–sIL-6Rα without interfering with the classical signaling pathway mediated by membrane-anchored IL-6Rα[14,15]. Soluble gp130 fully blocked the thermal induction of ICAM-1 expression on HEVs but did not prevent CCL21 upregulation (**Fig. 8a**). Moreover, disruption of IL-6 *trans* signaling by soluble gp130 prevented the thermal enhancement of HEV adhesion detected in frozen-section *in vitro* adherence assays as well as trafficking across HEVs *in vivo* without affecting the baseline activity of HEVs in normothermic conditions (**Fig. 8b**,**c**).

To determine whether thermal regulation of trafficking molecules in HEVs involves transcriptional control, we treated mice with actinomycin D, a pharmacological inhibitor of transcription *in vivo*[33]. We 'mapped' the requirement for transcriptional events in the IL-6 *trans*-signaling pathway leading to ICAM-1 induction in parallel studies that examined the effect of actinomycin D on IL-6 *trans*-signaling responses triggered directly by 'hyper-IL-6', a recombinant fusion protein in which IL-6 is covalently linked to sIL-6Rα[34]. We detected similar ICAM-1 induction on HEVs in response to hyper-IL-6 or thermal stress (**Fig. 8d**,**e**). However, in contrast to the site-specific response of thermal stress, ICAM-1 was also widely induced by hyper-IL-6 on vessels of extralymphoid organs (such as pancreas, liver, kidney and heart; **Fig. 8d** and data not shown). Actinomycin D abrogated ICAM-1 upregulation at all vascular sites in response to thermal stress or hyper-IL-6 (**Fig. 8e** and data not shown) without disrupting cellular processes that do not depend on new transcription, such as activation of 'downstream' signaling molecules (such as STAT3) by hyper-IL-6 (data not shown). The thermal enhancement of intravascular CCL21 in HEVs was also sensitive to actinomycin D treatment (**Fig. 8e**). Consistent with the observation that the thermal upregulation of CCL21 did not involve endogenous IL-6 *trans*-signaling mechanisms, administration of hyper-IL-6 failed to increase the presentation of CCL21 on HEVs (**Fig. 8e**). Overall, these data support a model whereby the vascular-specific effects of fever-range thermal stress on ICAM-1-mediated lymphocyte trafficking across HEVs are orchestrated by IL-6 *trans* signaling, whereas IL-6 is dispensable for enhanced intravascular display of CCL21 (**Supplementary Fig. 5** online).

## DISCUSSION

Secondary lymphoid organs are strategically positioned to provide the first line of defense against invading pathogens. Microbes entering the skin are a source of antigens that are transported by Langerhans cells to draining lymph nodes through the afferent lymphatics. These antigen-presenting cells localize proximal to HEVs[3], the main gateways for recirculating B lymphocytes and T lymphocytes. Enteric antigens have immediate access to gut-associated Peyer's patches and MLNs. The continual flux of pathogen-derived antigens and immune cells through lymphoid organs increases the probability that cognate antigens will be encountered by rare antigen-specific lymphocytes present at a frequency of only 1 in $1 \times 10^5$ to $1 \times 10^6$ cells.

Our study has provided insight into the beneficial mechanism of action of the thermal component of fever that has generally been relegated to a bystander function during infection and inflammation. A central finding was that fever-range thermal stress augmented the capture efficiency of gatekeeper HEVs for naive and central memory lymphocytes by increasing the intravascular density of CCL21 and ICAM-1. Notably, the approximately twofold increase in recruitment induced by thermal stress represented a profound enhancement in an already efficient process in which about one of every four lymphocytes that enter HEVs completes the multistep cascade leading to extravasation[1,3]. Thus, the acute effects of fever on lymphocyte trafficking would be predicted to enhance substantially the repertoire of antigen-specific B lymphocytes and T lymphocytes that screen lymphoid organs for the presence of foreign antigens. That mechanism complements the stimulatory effects of thermal stress on the migration of skin-derived Langerhans cells to lymph nodes[10,35].

Our findings expand on the long-recognized function of lymph nodes in mobilizing the immune system during inflammation[3,36]. Local release of TNF or CCL4 by mast cells at sites of bacterial challenge or antigen stimulation enhances T cell entry into draining lymph nodes[37,38]. Viral infection has also been reported to amplify $CD4^+$ and $CD8^+$ T cell recirculation by increasing the diameter of the feeding arterioles that supply postcapillary HEVs in draining lymph nodes (from about 100 μm to 150 μm)[39]. A fundamental difference between our findings and published results obtained in inflamed lymph nodes relates to the scope of the vascular response. Local inflammation at sites of infection or antigen challenge influences trafficking only in draining lymph nodes[3,36]. In contrast, fever-range WBH, which mirrors the thermal component of systemic fever, augments the recruitment properties of the 'HEV axis' throughout the body. Heightened immune surveillance of distal secondary lymphoid organs during fever would provide a substantial advantage by protecting the host against widespread dissemination of rapidly multiplying infectious agents. A notable distinction is that systemic thermal stress maintains homeostatic trafficking mechanisms, whereas local tissue inflammation 'opens the gateway' for $CCR7^-$ cell types normally excluded from trafficking across HEVs in draining lymph nodes[3,36]. Thus, thermal stress mainly improves the recruitment of naive and central memory $CD4^+$ and $CD8^+$ T cells and B cells across lymph node HEVs without disproportionately enhancing the homing of monocytes, neutrophils, effector-memory T cell subsets or activated T cells.

The maintenance of homeostatic lymphocyte recirculation by thermal stress is explained by the nature of the trafficking molecules upregulated on HEVs. Fever-range WBH 'preferentially' enhanced the intravascular density of two molecules involved in homeostatic trafficking (CCL21 and ICAM-1). Those data are consistent with *in vitro* studies showing that CCL21 and ICAM-1 act cooperatively to optimize LFA-1 binding activity[40–43]. CCL21 functions in a dose-dependent way *in vitro* to activate 'inside-out' signaling, leading to ligand-independent conformational changes that convert LFA-1 from a low-affinity state to an intermediate-affinity state[40,42]. Transition of LFA-1 to a high-affinity state depends on 'outside-in' signaling initiated by engagement of LFA-1 by ICAM-1 through a mechanism that is highly dependent on ICAM-1 density[40,41].

A central finding of our study was that CCL21 was necessary but not sufficient to support improved trafficking across HEVs in response to thermal stress. Interference with ICAM-1-dependent adhesion abrogated the thermal effects on trafficking despite high intravascular density of CCL21 and the availability of ICAM-2. The critical requirement for ICAM-1 during lymphocyte egress across HEVs demonstrated by thermal stress was unexpected, given that ICAM-1 and ICAM-2 can substitute for each other during steady-state trafficking in normothermic conditions[27,28]. Fundamental differences

between ICAM-1 and ICAM-2 may explain why ICAM-1 is the 'preferential' binding partner for LFA-1 during thermal responses. The high intravascular density of ICAM-1 resulting from thermal stimulation *in vivo* could theoretically favor the formation of stable dimers and higher-order multimers, as demonstrated biochemically in endothelial cells *in vitro* after ICAM-1 upregulation by TNF or by genetic overexpression[43,44]. Notably, ICAM-2 cannot form dimers, which may relate to intrinsic differences in the hydrophobicity of the N-terminal regions of ICAM-2 and ICAM-1 (refs. 43,45). ICAM-1 dimer formation reinforces molecular interactions with high-affinity LFA-1 conformers; thus, the bond lifetimes of monomeric and dimeric ICAM-1 for LFA-1 are about 25 s and 330 s, respectively[46]. The regulation of ICAM-1 density by thermal stress may also affect its ability to redistribute to cup-like structures that are proposed to provide traction for cells undergoing transmigration[47,48]. In contrast to ICAM-1, ICAM-2 is present in only moderate amounts in endothelial microdomains juxtaposed to LFA-1 on migrating lymphocytes[47].

Our studies here have demonstrated a nonredundant function for IL-6 *trans* signaling in controlling lymphocyte access to lymphoid organs during thermal stress. Disruption of IL-6 *trans*-signaling mechanisms prevented the thermal upregulation of ICAM-1 on HEVs and enhancement of lymphocyte homing. It remains to be determined if increased ICAM-1 expression results from the direct engagement of gp130 molecules on HECs by IL-6–sIL-6Rα and subsequent STAT3-mediated activation of the ICAM-1 promoter, as reported for primary endothelial cells (human umbilical vein endothelial cells) *in vitro*[30–32], or if other IL-6-responsive intermediary cells participate in that response. The finding that actinomycin D inhibited ICAM-1 upregulation on HEVs by both thermal stress and hyper-IL-6 indicated a transcriptional component of the pathway downstream of gp130 ligation by IL-6 and sIL-6Rα that controls new ICAM-1 synthesis. Our results excluding the possibility of involvement of IL-6–sIL-6Rα during thermal induction of the homeostatic chemokine CCL21 are not entirely unexpected, as IL-6 *trans* signaling has been linked mainly to regulation of the production of inflammatory chemokines (CCL2, CCL8, CXCL5 and CXCL6) *in vitro* or *in vivo*[14,15]. The mechanisms controlling CCL21 expression on the lumenal surface of HEVs are unknown[3,4]. Data indicating that the thermal control of intravascular presentation of CCL21 depended on newly initiated transcriptional events without altering the total nodal content of CCL21 are consistent with a scenario in which chemokine synthesis is induced only in limited cell populations (such as HECs or perivascular cells) or in which heat controls the transcription of as-yet-unidentified molecules involved in the transport, presentation or turnover of that homeostatic chemokine[3,4].

Many lines of evidence indicate that the IL-6 *trans*-signaling response initiated by thermal stress involves local microenvironmental control of adhesion in discrete vascular beds. Notably, the thermal effects on firm sticking of lymphocytes were restricted to high-order (III–V) venules (HEVs) in PLNs. That result was in contrast to studies demonstrating downstream low-order (I–II) segments in the same venular tree that were refractory to thermal stress. Immunolocalization studies established that upregulation of ICAM-1 occurred solely in the numerically minor population of HECs without affecting the total ICAM-1 content in nodal tissues. Moreover, ICAM-1 was not induced indiscriminately by hyperthermia in vessels of extralymphoid organs. A possible key to the tight control of vascular-specific responses lies in the dual requirement for IL-6 and sIL-6Rα in the initiation of thermal responses. Notably, the squamous endothelium of extralymphoid organs is able to upregulate ICAM-1 in response to IL-6 *trans* signaling initiated by hyper-IL-6. One possible explanation for the finding that thermal upregulation of ICAM-1 occurs exclusively in HEVs without affecting the overall IL-6 concentration in lymphoid organs is that site-specific vascular responses to hyperthermia are dictated by the local bioavailability of IL-6 and/or sIL-6R in microanatomically restricted sites. Many cell types are a potential source of IL-6 in lymphoid organs, including monocytes, lymphocytes, dendritic cells, endothelial cells, fibroblasts or pericytes located in the fibroreticular network surrounding HEVs, whereas sIL-6Rα derives mainly from leukocytes[13,49].

In conclusion, we have provided evidence that temperatures in the range of physiological fever act as an alert system to enhance the frequency of the homeostatic recirculation of lymphocytes across HEVs. The febrile response involves an integrated function for IL-6 *trans* signaling in controlling not only HEV adhesion, as reported here, but also the binding function of the L-selectin homing receptor in lymphocytes[9,13,17]. Our findings enlarge on the function of IL-6 *trans* signaling in controlling lymphocyte trafficking during acute and chronic inflammation[14,15]. IL-6–sIL-6Rα activity has been linked to T cell recruitment at sites of acute inflammation as well as to the pathogenesis of chronic inflammatory disorders, including inflammatory bowel disease, rheumatoid arthritis, peritonitis and diabetes[14,15]. Thus, our finding that IL-6 regulates ICAM-1-dependent lymphocyte trafficking in the context of acute febrile responses may have broad relevance to the mechanisms underlying chronic inflammation.

## METHODS

**Mice.** The following age-matched (8–12 weeks of age) female mice were purchased from Jackson Laboratory or Taconic: BALB/c, C3H, C57BL/6, severe combined immunodeficient (BALB/c background), IL-6-deficient (B6.129S2-*Il6*$^{tm1Kopf}$/J on a C57BL/6 background) and ICAM-1-deficient (Icam1$^{tmJegr}$/J on a C57BL/6 background). Mice were maintained in pathogen-free barrier conditions. All animal protocols were approved by the Roswell Park Cancer Institutional Animal Care and Use Committee.

**Treatment with fever-range WBH, cytokine-neutralizing reagents, recombinant cytokines or transcription inhibitor.** Mice were treated with fever-range WBH (core temperature of 39.5 ± 0.5 °C for 6 h) by being placed in an environmental chamber at 38.8 °C (model BE5000; Memmert) as described[16,35]. Normothermal control mice (core temperature, 36.8 ± 0.2 °C) were maintained at 22 °C in a darkened cabinet for the experimental period. Mice were injected intraperitoneally with 1 ml sterile saline to avoid dehydration, and the core temperatures of 'sentinel' mice in all experimental groups were monitored with a subcutaneously implanted microchip thermotransponder (14 mm × 2.2 mm; implanted 1 week or more before WBH treatment) and a programmable data-acquisition system (Bio Medic Data Systems). Neutralizing mAbs specific for IL-6, TNF, IL-1β, interferon-γ (100 μg/mouse in 200 μl PBS; R&D Systems) or recombinant soluble gp130 (2.5 μg/mouse in 250 μl PBS; R&D Systems) were injected intravenously into mice 30 min before WBH treatment. Mice were injected intraperitoneally with 1 ml of recombinant TNF (10 μg/kg body weight in sterile saline; R&D Systems) or hyper-IL-6 (80 μg/kg body weight) 6 h before organs were collected. Details for the production of hyper-IL-6 are in the **Supplementary Methods** online. Actinomycin D (Sigma) was injected intraperitoneally (2 mg/kg body weight in 1 ml saline, a dose reported to arrest transcription *in vivo*[33]) 30 min before the initiation of WBH or hyper-IL-6 treatment.

**Frozen-section *in vitro* adhesion assay.** Lymphocyte adhesion to HEVs was evaluated by a frozen-section *in vitro* adhesion assay as described[11,13,16]. A total of 5 × 10$^6$ mouse splenocytes were overlaid onto 12-μm-thick cryosections of PLNs (pooled inguinal, brachial, axillary, sciatic, superficial and deep cervical nodes) from normothermic control mice or WBH-treated mice. Selected lymphoid tissue specimens were blocked with mAb specific for PNAd (MECA79; 50 μg/ml), ICAM-1 (3E2; 5 μg/ml), ICAM-2 (3C4; 5 μg/ml) or isotype control antibody from BD Biosciences. The assay was done at 4 °C for 30 min with

mechanical rotation (112 r.p.m.; DS-500 Orbital Shaker; VWR). After removal of nonadherent cells, sections were fixed in 3% glutaraldehyde and were stained with 0.5% toluidine. Lymphocyte adhesion was quantified by light microscopy (Olympus, Spectra Services) for analysis of a total of $3 \times 10^2$ HEVs per lymphoid tissue sample. For consistency in 'double-blind' evaluations, HEVs were quantified only if they contained one adherent cell or more.

***In vivo* homing assay.** Homing of lymphocytes to lymphoid and nonlymphoid organs was assessed by a short-term homing assay[16,17]. Mouse splenocytes at a density of $5 \times 10^7$ cells per ml were labeled for 20 min at 37 °C with 180 μg/ml of TRITC (tetramethylrhodamine-6-isothiocyanate; Molecular Probes) or 1 μg/ml of calcein (Molecular Probes) in RPMI 1640 medium (Invitrogen), and labeling was stopped by centrifugation through a 'cushion' of FCS (Invitrogen). Equivalent numbers of labeled cells ($1 \times 10^7$ to $2 \times 10^7$ cells in 300 μl PBS) were injected intravenously into WBH-treated mice and normothermic control mice, and organs were collected 1 h after cell transfer unless otherwise indicated. PLNs consisted of pooled inguinal, brachial, axillary, sciatic, superficial and deep cervical nodes. The number of fluorescence-labeled cells was quantified (by researchers 'blinded' to sample identity) with a BH2/RFL fluorescence microscope (Olympus Optical) in ten fields or more (unit area of each field, 0.34 $mm^2$) of nonsequential cryosections 9 μm in thickness. The percentage of fluorescence-labeled cells in single-cell suspensions of recipient lymphoid organs was also analyzed by flow cytometry with a FACScan (BD Biosciences). Equivalent results were obtained by microscopic quantification and flow cytometry; all results were confirmed by both methods. The constant ratio (about 1:1) of transferred cells in spleens of control mice and WBH-treated mice provided an internal reference standard for the number of input cells in homing studies. Details of treatment with adhesion-blocking antibodies, chemokines and pertussis toxin are provided in the **Supplementary Methods**. For studies involving the homing of an enriched population of $CD4^+$ or $CD8^+$ T cells that was L-selectin-low, $CXCR3^{hi}$, mouse splenocytes were activated for 2 d *in vitro* with plate-bound mAb to mouse CD3 (145-2C11; BD Biosciences), followed by treatment for 3 d with recombinant IL-2 (12.5 ng/ml; R&D Systems)[50].

**Flow cytometry.** Multiparameter flow cytometry was used for 'phenotyping' of TRITC-labeled cells before or after transfer in single-cell suspensions of PLNs and spleen from recipient mice. Details are provided in the **Supplementary Methods**.

**Intravital microscopy.** Intravital microscopy of inguinal PLNs was done as described[17,23]. C57BL/6 mice were anesthetized by intraperitoneal injection of 1 mg/ml of xylazine and 10 mg/ml of ketamine (10 ml per kg body weight). The left inguinal lymph node was exposed in an abdominal skin flap and the surrounding fatty tissue was removed to expose the lymph node microvasculature. Approximately $2.5 \times 10^7$ calcein-labeled splenocytes were injected through a catheter inserted into the right femoral artery and were visualized with a customized intravital microscopy system (Spectra Services). Brightfield microscopy was used to identify the vascular structure and blood flow status in venular branches; fluorescent microscopy was used to visualize calcein-labeled cells. At the end of the observation period, 150-kilodalton fluorescein isothiocyanate–conjugated dextran (10 mg/ml; Molecular Probes) was injected to define the venular structure. All images were captured with an EB charge-coupled device camera (Hamamatsu Photonics) and were recorded with a digital videocassette recorder (DSR-11, Sony) for analysis of cell activity. The rolling fraction was defined as the percentage of total cells passing through the vessel that transiently interacted with HEVs during the observation period[17,23]. The sticking fraction was defined as the percentage of rolling cells that adhered to HEVs for 30 s or more. For rolling and sticking fractions, data were generated from three normothermic control mice (venules analyzed: order I, 3; order II, 8; order III, 15; order IV, 16; order V, 12) and three WBH-treated mice (venules analyzed: order I, 4; order II, 7; order III, 11; order IV, 13; order V, 11). The velocity of more than 20 noninteracting (fast-moving) cells in order III venules was measured in each mouse.

**Immunofluorescence analysis.** Organs were embedded in optimum cutting temperature compound (Sakura Finetek). Tissue cryosections 9 μm in thickness were fixed for 10 min at –20 °C in methanol/acetone (3:1), and the expression of homing molecules was detected by immunofluorescence staining. Details of the procedures for staining of organ cryosections or intravascular staining are in the **Supplementary Methods**. Digital images were captured with an Olympus BX50 upright fluorescence microscope equipped with a SPOT RT camera (Spectra Services). Confocal images were obtained with the Leica TCS SP2 spectrophotometer confocal microscope. All images were captured with identical exposure times and image settings in each experiment. Images were analyzed with ImageJ software[51] (http://rsb.info.nih.gov/ij) for determination of the relative fluorescence staining intensity for trafficking molecules on all HEVs in a single 9-μm-thick cross-section of 14 pooled PLNs (paired inguinal, brachial, axillary, sciatic, superficial and deep cervical nodes). For normalization of the varying sizes of individual HEVs in cryosections, fluorescence intensity is expressed in terms of pixels (reflecting a fixed unit area). For this, $PNAd^+$ cuboidal structures were circled (with Intuos3 USB Pen Tablet; Wacom) and each pixel in those defined regions was assigned a fluorescence intensity value (based on a scale from 0 to 255). Histograms represent the data from all pixels analyzed (range, $1 \times 10^6$ to $1.7 \times 10^6$) for the total HEVs per cryosection (range, $1 \times 10^2$ to $1.75 \times 10^2$); similar numbers of HEVs and pixels were analyzed for each treatment condition in individual experiments.

**Immunoblots and enzyme-linked immunosorbent assay.** PLNs were sonicated to obtain total tissue lysates. For immunoblot analysis of CCL21, equal amounts of protein (20 μg) were fractionated by reducing SDS-PAGE (12% acrylamide), and membrane blots were probed with antibodies specific for CCL21 (R&D Systems) or β-actin (Sigma). Recombinant CCL21 (R&D Systems) was used as a positive control. ICAM-1 protein in PLN tissue lysates was measured by enzyme-linked immunosorbent assay (R&D Systems). IL-6 concentrations in PLN tissue lysates were measured by multiplex immunoassay (Luminex 100) using mouse Fluorokine MAP assays (R&D Systems). Phosphorylated STAT3 was detected by immunoblot analysis[13] in liver and spleen extracts of mice pretreated with actinomycin D for various times (0, 0.5, 1, 2 and 4 h), followed by 30 min of treatment with hyper-IL-6.

**Statistical analysis.** Statistical analysis used the unpaired, two-tailed Student's *t*-test.

*Note: Supplementary information is available on the Nature Immunology website.*


## ACKNOWLEDGMENTS

We thank J.D. Black and E.A. Repasky for discussions and comments on the manuscript; M. Miyasaka and T. Tanaka (Osaka University) for antiserum to mouse Duffy antigen–related receptor for chemokines; P.K. Wallace and E.A. Timm for assistance with flow cytometry of leukocyte subsets; and E.L. Hurley for technical support for confocal microscopy. Supported by the US National Institutes of Health (CA79765 and CA094045 to S.S.E.; AI061663 and AI069259 to U.V.A.; DK33886 and CA85580 to H.B.; and CA16056 to Roswell Park Cancer Institute), the Department of Defense (W81XWH-04-1-0354 to Q.C.), the Roswell Park Alliance Foundation (to S.S.E.), the Leukocyte Migration Core of the Harvard Skin Disease Research Center (P30 AR 42689 to U.H.v.A.) and the Deutsche Forschungsgemeinschaft (Bonn, Germany; SFB414, TPB5 to S.R.J.).


## AUTHOR CONTRIBUTIONS

Q.C. and S.S.E. conceptualized and designed the research; S.S.E. supervised the research; Q.C. did all experiments unless stated otherwise; D.T.F. contributed to the experimental design for quantitative image analysis and did the phenotypic analysis in short-term homing assays and enzyme-linked immunosorbent assay for ICAM-1; K.A.C assisted in immunofluorescence staining and kinetic analysis in short-term homing assays; E.U. contributed to the analysis of ICAM-1 staining; W.-C.W. did frozen-section adherence assays and provided technical assistance for organ retrieval; U.H.v.A. and J.-M.G. helped with intravital microscopy studies; S.R.J. provided the hyper-IL-6 expression construct; H.B. provided recombinant hyper-IL-6 and contributed to discussions regarding IL-6 regulation of lymphocyte trafficking; and all authors contributed to discussions and to the preparation of the manuscript.

## COMPETING INTERESTS STATEMENT

The authors declare that they have no competing financial interests.

Published online at http://www.nature.com/natureimmunology/
Reprints and permissions information is available online at http://npg.nature.com/reprintsandpermissions/




1. Girard, J.P. & Springer, T.A. High endothelial venules (HEVs): specialized endothelium for lymphocyte migration. *Immunol. Today* **16**, 449–457 (1995).
2. Butcher, E.C. & Picker, L.J. Lymphocyte homing and homeostasis. *Science* **272**, 60–66 (1996).
3. von Andrian, U.H. & Mempel, T.R. Homing and cellular traffic in lymph nodes. *Nat. Rev. Immunol.* **3**, 867–878 (2003).
4. Miyasaka, M. & Tanaka, T. Lymphocyte trafficking across high endothelial venules: dogmas and enigmas. *Nat. Rev. Immunol.* **4**, 360–370 (2004).
5. Rosen, S.D. Ligands for L-selectin: homing, inflammation, and beyond. *Annu. Rev. Immunol.* **22**, 129–156 (2004).
6. Engelhardt, B. & Wolburg, H. Mini-review: Transendothelial migration of leukocytes: through the front door or around the side of the house? *Eur. J. Immunol.* **34**, 2955–2963 (2004).
7. Kluger, M.J. Fever: role of pyrogens and cryogens. *Physiol. Rev.* **71**, 93–127 (1991).
8. Hasday, J.D., Fairchild, K.D. & Shanholtz, C. The role of fever in the infected host. *Microbes Infect.* **2**, 1891–1904 (2000).
9. Appenheimer, M.M., Chen, Q., Girard, R., Wang, W.C. & Evans, S.S. Impact of fever-range thermal stress on lymphocyte-endothelial adhesion and lymphcoyte trafficking. *Immunol. Invest.* **34**, 295–323 (2005).
10. Ostberg, J.R. & Repasky, E.A. Emerging evidence indicates that physiologically relevant thermal stress regulates dendritic cell function. *Cancer Immunol. Immunother.* **55**, 292–298 (2006).
11. Wang, W.C. *et al.* Fever-range hyperthermia enhances L-selectin-dependent adhesion of lymphocytes to vascular endothelium. *J. Immunol.* **160**, 961–969 (1998).
12. Evans, S.S., Bain, M.D. & Wang, W.C. Fever-range hyperthermia stimulates $\alpha_4\beta_7$ integrin-dependent lymphocyte-endothelial adhesion. *Int. J. Hyperthermia* **16**, 45–59 (2000).
13. Chen, Q. *et al.* Central role of IL-6 receptor signal-transducing chain gp130 in activation of L-selectin adhesion by fever-range thermal stress. *Immunity* **20**, 59–70 (2004).
14. Jones, S.A. Directing transition from innate to acquired immunity: defining a role for IL-6. *J. Immunol.* **175**, 3463–3468 (2005).
15. Jones, S.A. & Rose-John, S. The role of soluble receptors in cytokine biology: the agonistic properties of the sIL-6R/IL-6 complex. *Biochim. Biophys. Acta* **1592**, 251–263 (2002).
16. Evans, S.S. *et al.* Fever-range hyperthermia dynamically regulates lymphocyte delivery to high endothelial venules. *Blood* **97**, 2727–2733 (2001).
17. Chen, Q., Fisher, D.T., Kucinska, S.A., Wang, W.C. & Evans, S.S. Dynamic control of lymphocyte trafficking by fever-range thermal stress. *Cancer Immunol. Immunother.* **55**, 299–311 (2006).
18. Shah, A. *et al.* Cytokine and adhesion molecule expression in primary human endothelial cells stimulated with fever-range hyperthermia. *Int. J. Hyperthermia* **18**, 534–551 (2002).
19. Hasday, J.D. *et al.* Exposure to febrile temperature modifies endothelial cell response to tumor necrosis factor-$\alpha$. *J. Appl. Physiol.* **90**, 90–98 (2001).
20. Choi, J., Enis, D.R., Koh, K.P., Shiao, S.L. & Pober, J.S. T lymphocyte-endothelial cell interactions. *Annu. Rev. Immunol.* **22**, 683–709 (2004).
21. Gauguet, J.M., Rosen, S.D., Marth, J.D. & von Andrian, U.H. Core 2 branching $\beta$1,6-N-acetylglucosaminyltransferase and high endothelial cell N-acetylglucosamine-6-sulfotransferase exert differential control over B- and T-lymphocyte homing to peripheral lymph nodes. *Blood* **104**, 4104–4112 (2004).
22. Stevens, S.K., Weissman, I.L. & Butcher, E.C. Differences in the migration of B and T lymphocytes: organ-selective localization *in vivo* and the role of lymphocyte-endothelial cell recognition. *J. Immunol.* **128**, 844–851 (1982).
23. von Andrian, U.H. Intravital microscopy of the peripheral lymph node microcirculation in mice. *Microcirculation* **3**, 287–300 (1996).
24. Kashiwazaki, M. *et al.* A high endothelial venule-expressing promiscuous chemokine receptor DARC can bind inflammatory, but not lymphoid, chemokines and is dispensable for lymphocyte homing under physiological conditions. *Int. Immunol.* **15**, 1219–1227 (2003).
25. Izawa, D. *et al.* Expression profile of active genes in mouse lymph node high endothelial cells. *Int. Immunol.* **11**, 1989–1998 (1999).
26. Okada, T. *et al.* Chemokine requirements for B cell entry to lymph nodes and Peyer's patches. *J. Exp. Med.* **196**, 65–75 (2002).
27. Lehmann, J.C. *et al.* Overlapping and selective roles of endothelial intercellular adhesion molecule-1 (ICAM-1) and ICAM-2 in lymphocyte trafficking. *J. Immunol.* **171**, 2588–2593 (2003).
28. Gerwin, N. *et al.* Prolonged eosinophil accumulation in allergic lung interstitium of ICAM-2 deficient mice results in extended hyperresponsiveness. *Immunity* **10**, 9–19 (1999).
29. McEvoy, L.M., Jutila, M.A., Tsao, P.S., Cooke, J.P. & Butcher, E.C. Anti-CD43 inhibits monocyte-endothelial adhesion in inflammation and atherogenesis. *Blood* **90**, 3587–3594 (1997).
30. Roebuck, K.A. & Finnegan, A. Regulation of intercellular adhesion molecule-1 (CD54) gene expression. *J. Leukoc. Biol.* **66**, 876–888 (1999).
31. Modur, V., Li, Y., Zimmerman, G.A., Prescott, S.M. & McIntyre, T.M. Retrograde inflammatory signaling from neutrophils to endothelial cells by soluble interleukin-6 receptor $\alpha$. *J. Clin. Invest.* **100**, 2752–2756 (1997).
32. Romano, M. *et al.* Role of IL-6 and its soluble receptor in induction of chemokines and leukocyte recruitment. *Immunity* **6**, 315–325 (1997).
33. Bergo, M., Wu, G., Ruge, T. & Olivecrona, T. Down-regulation of adipose tissue lipoprotein lipase during fasting requires that a gene, separate from the lipase gene, is switched on. *J. Biol. Chem.* **277**, 11927–11932 (2002).
34. Fischer, M. *et al.* I. A bioactive designer cytokine for human hematopoietic progenitor cell expansion. *Nat. Biotechnol.* **15**, 142–145 (1997).
35. Ostberg, J.R., Gellin, C., Patel, R. & Repasky, E.A. Regulatory potential of fever-range whole body hyperthermia on Langerhans cells and lymphocytes in an antigen-dependent cellular immune response. *J. Immunol.* **167**, 2666–2670 (2001).
36. Sallusto, F. & Mackay, C.R. Chemoattractants and their receptors in homeostasis and inflammation. *Curr. Opin. Immunol.* **16**, 724–731 (2004).
37. Mackay, C.R., Marston, W. & Dudler, L. Altered patterns of T cell migration through lymph nodes and skin following antigen challenge. *Eur. J. Immunol.* **22**, 2205–2210 (1992).
38. Tedla, N. *et al.* Regulation of T lymphocyte trafficking into lymph nodes during an immune response by the chemokines macrophage inflammatory protein (MIP)-1$\alpha$ and MIP-1$\beta$. *J. Immunol.* **161**, 5663–5672 (1998).
39. Soderberg, K.A. *et al.* Innate control of adaptive immunity via remodeling of lymph node feed arteriole. *Proc. Natl. Acad. Sci. USA* **102**, 16315–16320 (2005).
40. Carman, C.V. & Springer, T.A. Integrin avidity regulation: are changes in affinity and conformation underemphasized? *Curr. Opin. Cell Biol.* **15**, 547–556 (2003).
41. Shamri, R. *et al.* Lymphocyte arrest requires instantaneous induction of an extended LFA-1 conformation mediated by endothelium-bound chemokines. *Nat. Immunol.* **6**, 497–506 (2005).
42. Pachynski, R.K., Wu, S.W., Gunn, M.D. & Erle, D.J. Secondary lymphoid-tissue chemokine (SLC) stimulates integrin $\alpha_4\beta_7$-mediated adhesion of lymphocytes to mucosal addressin cell adhesion molecule-1 (MAdCAM-1) under flow. *J. Immunol.* **161**, 952–956 (1998).
43. Reilly, P.L. *et al.* The native structure of intercellular adhesion molecule-1 (ICAM-1) is a dimer. Correlation with binding to LFA-1. *J. Immunol.* **155**, 529–532 (1995).
44. Miller, J. *et al.* Intercellular adhesion molecule-1 dimerization and its consequences for adhesion mediated by lymphocyte function associated-1. *J. Exp. Med.* **182**, 1231–1241 (1995).
45. Casasnovas, J.M., Stehle, T., Liu, J.H., Wang, J.H. & Springer, T.A. A dimeric crystal structure for the N-terminal two domains of intercellular adhesion molecule-1. *Proc. Natl. Acad. Sci. USA* **95**, 4134–4139 (1998).
46. Sarantos, M.R., Raychaudhuri, S., Lum, A.F., Staunton, D.E. & Simon, S.I. Leukocyte function-associated antigen 1-mediated adhesion stability is dynamically regulated through affinity and valency during bond formation with intercellular adhesion molecule-1. *J. Biol. Chem.* **280**, 28290–28298 (2005).
47. Carman, C.V. & Springer, T.A. A transmigratory cup in leukocyte diapedesis both through individual vascular endothelial cells and between them. *J. Cell Biol.* **167**, 377–388 (2004).
48. Shaw, S.K. *et al.* Coordinated redistribution of leukocyte LFA-1 and endothelial cell ICAM-1 accompany neutrophil transmigration. *J. Exp. Med.* **200**, 1571–1580 (2004).
49. Naka, T., Nishimoto, N. & Kishimoto, T. The paradigm of IL-6: from basic science to medicine. *Arthritis Res.* **4**, S233–S242 (2002).
50. Weninger, W., Crowley, M.A., Manjunath, N. & von Andrian, U.H. Migratory properties of naive, effector, and memory $CD8^+$ T cells. *J. Exp. Med.* **194**, 953–966 (2001).
51. Abramoff, M.D., Magelhaes, P.J. & Ram, S.J. Image processing with ImageJ. *Biophotonics Int.* **11**, 36–42 (2004).

# Erratum: Fever-range thermal stress promotes lymphocyte trafficking across high endothelial venules via an interleukin 6 *trans*-signaling mechanism

**Qing Chen, Daniel T Fisher, Kristen A Clancy, Jean-Marc M Gauguet, Wan-Chao Wang, Emily Unger, Stefan Rose-John, Ulrich H von Andrian, Heinz Baumann & Sharon S Evans**

*Nat. Immunol.*, **doi:10.1038/ni1406; corrected 10 November 2006**

In the version of this article initially published online, the label for the bottom row of **Figure 8d** is missing. It should read 'H-IL-6'. The error has been corrected for all versions of the article.